DOI: 10.1002/cphc.200700502

A Crossed Molecular Beam Study on the Reaction of Boron Atoms with Methylacetylene and Partially Deuterated Methylacetylene

Fangtong Zhang,[a] Chih Hao Kao,[b] Agnes H. H. Chang,[b] Xibin Gu,[a] Ying Guo,[a] and Ralf I. Kaiser*[a]

The reactions of ground-state boron atoms, $B(^2P_j)$, with methylacetylene, $CH_3CCH(X^1A_1)$, and its [D3]-substituted isotopomer, $CD_3CCH(X^1A_1)$, are studied under single collision conditions using the crossed molecular beam technique at collision energies of 21.6 and 21.9 kJ mol^{-1}, respectively. Utilizing the CD_3CCH reactant, detailed information on the dynamics is obtained. The reaction followed indirect scattering dynamics and proceeded through at least two reaction channels via atomic deuterium and hydrogen atom elimination pathways leading eventually to two isotopomers, that is, the C_{2v} symmetric $D_2CCCBH(X^1A_1)$ and $D_2CCCBD(X^1A_1)$ structures via statistical and non-statistical reaction pathways, respectively.

1. Introduction

Due to its high energy density, both in volume and gravity terms,[1,2] boron has long been regarded as a good candidate for rocket fuel additives.[3–6] To fulfill this potential, it is essential to understand the boron combustion chemistry and the reactions of boron atoms with hydrocarbon fuels on the molecular level. Therefore, elementary reactions of ground-state boron atoms, $B(^2P_j)$, with unsaturated hydrocarbons and the thermodynamical properties of boron-substituted hydrocarbons have been investigated both experimentally and theoretically. Before experimental data became available, theoreticians had predicted that the cyclic, 2π-Hückel aromatic compound borirene, $(CH)_2BH$, is thermodynamically stable [Figure 1, (1)].[7–10] Efforts have also been made to understand the effect of boron-substitution and insertion reactions into hydrocarbon molecules.[11–15] For instance, Andrews and co-workers successfully conducted the reactions of boron atoms with acetylene,[16–18] ethylene,[19,20] and ethane[20] utilizing the matrix isolation and infrared (IR) spectroscopy coupled with theoretical calculations on the normal modes of the newly formed molecules.[21] Among their pioneering achievements was the identification of the elusive borirene molecule via low-temperature spectroscopy. However, since the boron atoms were generated via free-laser ablation, the electronic states of the reacting boron atoms could not be determined; hence, the authors were unable to elucidate the reaction mechanism(s).

This problem was finally solved in a crossed beams reaction of ground-state boron atoms with ethylene by providing a true single collision environment where it was possible to observe the consequences of a single reactive event.[22] In 2000, Balucani et al. investigated the reaction of laser-ablated boron atoms with ethylene[22] and successfully formed the elusive cyclic borirene (1), the smallest neutral aromatic molecule, in the gas phase (Figure 1). Based upon their results, borirene was found to be formed via the addition of a ground-state boron atom, $B(^2P_j)$, to the π bond of the ethylene (C_2H_4) molecule yielding a borirane radical intermediate. The latter underwent a hydrogen migration from the carbon to the boron atom followed by an atomic hydrogen loss from the methylene group to eventually synthesize borirene. The boron atom insertion into a C–H bond pathway was concluded to be energetically inaccessible for ground-state boron atoms. Successively, Balucani et al. investigated the reaction of ground-state boron atoms with acetylene under single collision conditions.[23,24] Contradictory to some early theoretical calculation, the experiments demonstrated that only the boron versus

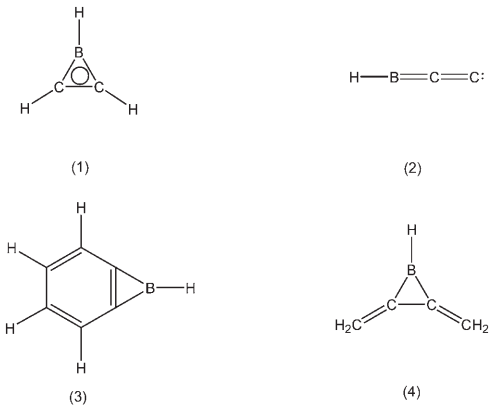

Figure 1. Structures of the reaction products of ground-state boron atoms with ethylene, acetylene, benzene, and dimethylacetylene.

[a] Dr. F. Zhang, Dr. X. Gu, Dr. Y. Guo, Prof. R. I. Kaiser
Department of Chemistry, University of Hawaii
Honolulu, HI 96822 (USA)
Fax: (+1) 808-956-5908
E-mail: ralfk@hawaii.edu

[b] Prof. C. H. Kao, Prof. A. H. H. Chang
Department of Chemistry, National Dong Hwa University
Hualien, 974 (Taiwan)

atomic hydrogen exchange channel is open. The reaction dynamics were suggested to be indirect, proceeded via addition of the boron atom to the carbon–carbon triple bond via a cyclic intermediate, and formed—after successive isomerizations and a hydrogen elimination—the linear HBCC($X^1\Sigma_g^+$) isomer [Figure 1, (2)]. The third boron reaction studied in crossed beams experiments was that with benzene (C_6H_6) and [D6]benzene (C_6D_6).[25–27] After successive isomerization and rearrangements of the initial addition complex, an atomic hydrogen/deuterium elimination yielded the [D5]benzoborirene molecule [Figure 1; (3)]. Again, an insertion into a carbon–hydrogen bond was not feasible. Finally, Sillars et al. reported results of the reaction of ground-state boron, $B(^2P_j)$ with dimethylacetylene, $CH_3CCCH_3(X^1A_{1g})$.[28] It was found that the reaction followed indirect scattering dynamics; $B(^2P_j)$ attacked the carbon–carbon triple bond of the dimethylacetylene molecule to a cyclic BC_4H_6 intermediate that underwent hydrogen transfer from the methyl group to the boron atom. This complex then fragmented via atomic hydrogen emission to a cyclic BC_4H_5 isomer, 1,2-dimethylene-3-bora-cyclopropane, via a tight exit transition state [Figure 1, (4)].

These studies investigated the role of acetylene, ethylene and benzene as prototype reaction partners of molecules containing triple, double, and "aromatic" bonds. An experimental study of the reaction of ground-state boron atoms with methylacetylene [$CH_3CCH(X^1A_1)$] would bridge the previous crossed beam experiments of atomic boron with acetylene and dimethylacetylene. To the best of our knowledge, there has been neither an experimental nor theoretical study on the boron–methylacetylene system to date. Therefore, in this paper we will report the first results of elementary boron reaction with methylacetylene and its partially deuterated [D3]methylacetylene isotopomer (CD_3CCH); the latter is important to pin down the position of a potential hydrogen–deuterium loss to answer the question to what extent the atomic hydrogen/deuterium loss originates from the methyl and/or from the acetylenic group. Our studies will also give insights into the hitherto poorly explored BC_3H_3 and BC_3H_4 potential energy surfaces (PESs).[29]

Experimental Section

The elementary reaction of ground-state boron atoms, $B(^2P_j)$, with methylacetylene, $CH_3CCH(X^1A_1)$ was conducted in a universal crossed molecular beams machine under single collision conditions at the University of Hawaii. The experimental setup has been described in detail elsewhere.[30–32] Briefly, a pulsed boron atom beam was generated in the primary source chamber by laser ablation of a boron rod at 266 nm (30 Hz; 5 ~ 10 mJ per pulse).[33] The ablated species were seeded in neat carrier gas (helium, 99.9999 %, Airgas) released by a Proch-Trickl pulsed valve at 4 atm backing pressure. It is important to stress that the boron beam is pulsed. Consequently, different parts of the boron beam have distinct peak velocities and speed ratios. Therefore, after passing a skimmer, a four-slot chopper wheel selected a part out of the boron beam at a peak velocity, v_p of 2070 ± 10 ms^{-1}; speed ratios of 3.5 ± 0.2 were obtained (Table 1). Note that the ablation beam contains both ^{11}B (80 %) and ^{10}B (20 %) species in their natural abundances. This has to be considered in the fits of the laboratory data. The experimental conditions such as the delay times between the laser and the pulsed valve as well as the laser power and laser focus were optimized so that no metastable boron atoms exist in the beam. The segment of the boron beam crossed a pulsed methylacetylene beam (CH_3CCH, 99.9 %, Organic Technologies; 550 torr) or partially deuterated methylacetylene beam (CD_3CCH, 99.8 % deuterium enrichment, CDN Isotopes; 350 torr), released by a second pulsed valve perpendicularly in the interaction region.

Table 1. Peak velocities (v_p) of the segments of the crossing beams, their speed ratios (S) and the center-of-mass angles calculated for the ^{11}B isotope (Θ_{CM}), together with the nominal collision energies (E_c) of the boron–methylacetylene and boron–[D3]methylacetylene systems. The speed ratio is defined via Equation (1) with $\alpha = [(2RT)/m]^{-1/2}$ with m being the mass of the species, R the ideal gas constant, and T the temperature of the beam.

Beam	v_p [ms^{-1}]	S	E_c [kJ mol^{-1}]	Θ_{CM}
$CH_3CCH(X^1A_1)$	840 ± 3	9.0 ± 1.0	–	–
$B(^2P_j)$/He	2072 ± 7	3.5 ± 0.1	21.6 ± 0.1	55.8 ± 0.1
$CD_3CCH(X^1A_1)$	840 ± 3	9.0 ± 1.0	–	–
$B(^2P_j)$/He	2071 ± 8	3.5 ± 0.1	21.9 ± 0.1	57.8 ± 0.1

The reactively scattered species were monitored using a quadrupole mass spectrometric detector in the time-of-flight (TOF) mode after electron-impact ionization of the molecules. This detector can be rotated within the plane defined by the primary and the secondary reactant beams to facilitate the acquisition of angular resolved TOF spectra. At each angle, 300 000 TOF spectra were accumulated to obtain good signal to noise ratios. The recorded TOF spectra were then integrated and normalized to extract the product angular distribution in the laboratory frame (LAB). To collect information on the scattering dynamics, the laboratory data were transformed into the center-of-mass reference frame utilizing a forward-convolution routine.[34,35] This iterative method initially guesses the angular flux distribution, $T(\theta)$, and the translational energy flux distribution, $P(E_T)$ in the center-of-mass system (CM). Laboratory TOF spectra and the laboratory angular distributions (LAB) were then calculated from the $T(\theta)$ and $P(E_T)$ functions and were averaged over a grid of Newton diagrams. Each diagram defines, for instance, the velocity and angular spread of each beam and the detector acceptance angle. Best fits were obtained by iteratively refining the adjustable parameters in the center-of-mass functions [Eq. (1)].

$$N(v) = v^2 \exp\left[-\left(\frac{v}{\alpha} - S\right)^2\right] \quad (1)$$

2. Results

2.1. Reactive Scattering Signal

In the case of the $B(^2P_j)$–$CH_3CCH(X^1A_1)$ system, the reactive scattering signal was monitored in the range of mass-to-charge ratios, m/z, from 50 to 46. Here, the signal at $m/z = 50$ originated from $^{11}BC_3H_3^+$, at $m/z = 49$ from $^{11}BC_3H_2^+$ and $^{10}BC_3H_3^+$, $m/z = 48$ from $^{11}BC_3H^+$ and $^{10}BC_3H_2^+$, $m/z = 47$ from $^{11}BC_3^+$ and $^{10}BC_3H^+$, and $m/z = 46$ from $^{10}BC_3^+$. At each angle, the TOFs of these ions are—after scaling—superimposable, indicating that the signal at lower m/z ratios originated from dissociative ionization of the parent molecules in the electron

impact ionizer. This finding alone implies that the boron versus hydrogen atom exchange pathway is open. We would like to stress that no reactive scattering signal association to $BC_3H_4^+$ ($m/z=51$) or higher masses were detected. Consequently, data were acquired at $m/z=50$ because of the highest signal-to-noise ratio at this mass-to-charge ratio (Figure 2). The corresponding LAB distribution is shown in Figure 3. Note that the

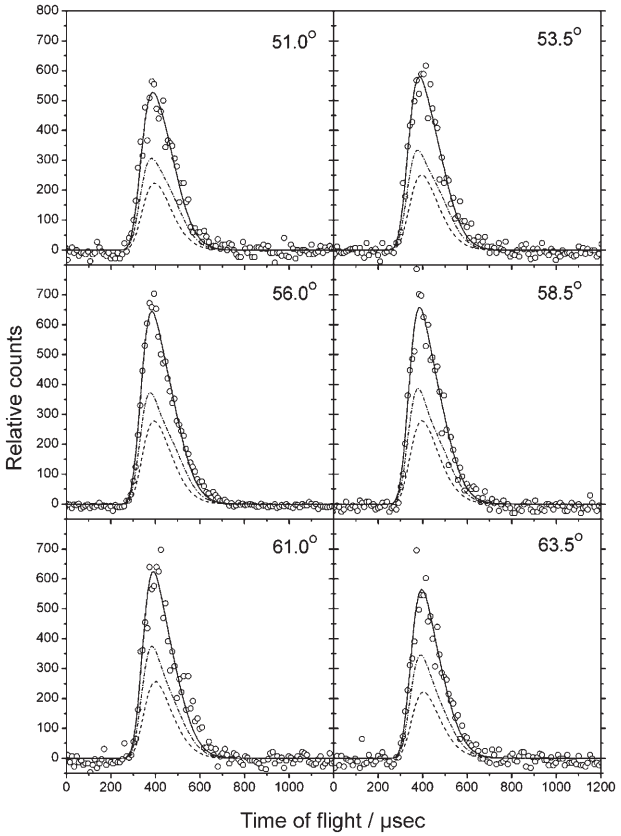

Figure 2. Time-of-flight data at $m/z=50$ recorded for the reaction $^{11}B(^2P_j)+CH_3CCH(X^1A_1)$ at various laboratory angles at a collision energy of 21.6 kJ mol^{-1}. The circles represent the experimental data, and the solid line represents the fit. The two dashed lines represent the two microchannels. Each TOF spectrum has been normalized to the relative intensity of each angle.

laboratory angular distribution of the heavy reaction product of the generic formula $^{11}BC_3H_3$ is forward-backward symmetric, peaks around 55° close to the center-of-mass angle of 55.8± 0.1°, and is spread at least 45° degrees within the scattering plane. The shape of the LAB distribution suggests that the reaction proceeds via indirect scattering dynamics involving $^{11}BC_3H_4$ reaction intermediate(s). We would like to comment briefly on the influence of the ^{10}B isotope on the shape of the TOF spectra and on the LAB distributions. Based on the center-of-mass angles of the $^{11}B(^2P_j)$–$CH_3CCH(X^1A_1)$ versus $^{10}B(^2P_j)$–$CH_3CCH(X^1A_1)$ systems of 55.8° and 58.3°, we would expect an offset of the laboratory angular distributions of $m/z=50$ originating from $^{11}BC_3H_3^+$ and $m/z=49$ from $^{11}BC_3H_2^+$ and $^{10}BC_3H_3^+$ by about 2.5°. However, the strongly exoergic nature of the reaction together with the velocity and angular spread of the boron atom beam wash out this effect in the boron–methylacetylene system. However, this offset has been observed in the $^{11/10}B/CD_3CCH$ system by comparing the H versus D atom loss pathway from the acetylenic and methyl group. Here, the extended scattering range as defined by the Newton circle of the deuterium atom loss pathway compared to the hydrogen atom loss shows the offset explicitly.

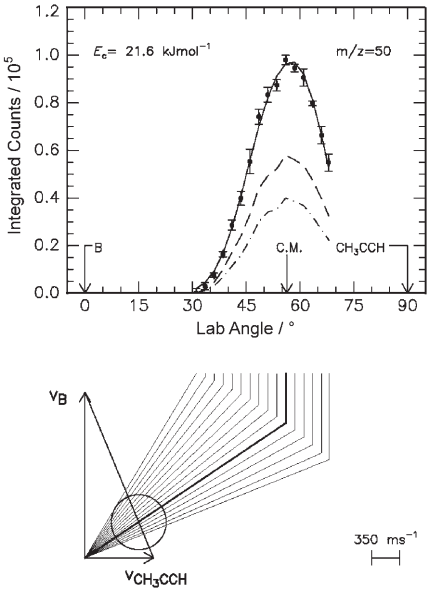

Figure 3. Lower panel: Newton diagram for the reaction $^{11}B(^2P_j)+CH_3CCH(X^1A_1)$ at a collision energy of 21.6 kJ mol^{-1}. Upper panel: Laboratory angular distribution of the $^{11}BC_3H_3$ product at $m/z=50$. Circles and 1σ error bars indicate experimental data, the solid line indicates the calculated distribution and the dashed lines represent two micro-channels. The center-of-mass angle is indicated by C.M. The solid lines originating in the Newton diagram point to distinct laboratory angles whose times of flight are shown in Figure 2.

Having identified the atomic hydrogen loss pathway, it is important to derive experimentally to what extent the hydrogen atom originates from the methyl group and/or from the acetylenic group. Therefore, we conducted experiments with [D3]methylacetylene [$CD_3CCH(X^1A_1)$]. Based on the LAB distribution of the $B(^2P_j)$–$CH_3CCH(X^1A_1)$ system, we expect also indirect scattering dynamics and the formation of $^{11}BCD_3CCH$ and $^{10}BCD_3CCH$ intermediates (Figure 4). Considering the parent ions, an atomic hydrogen emission from the reaction intermediates would result in a signal at $m/z=53$ ($^{11}BC_3D_3^+$) and $m/z=52$ ($^{10}BC_3D_3^+$). The neutral products can fragment in the electron impact ionizer to yield $m/z=51$ ($^{11}BC_3D_2^+$) and $m/z=50$ ($^{10}BC_3D_2^+$). In the case of a deuterium loss, the signal of the ionized parent molecules should be present at $m/z=52$ ($^{11}BC_3D_2H^+$) and $m/z=51$ ($^{10}BC_3D_2H^+$). Also, these parent molecules are expected to show fragment ions at $m/z=51$ ($^{11}BC_3D_2^+$), $m/z=50$ ($^{11}BC_3DH^+/^{10}BC_3D_2^+$), and $m/z=49$ ($^{10}BC_3DH^+$). Figure 4 summarizes the expected pattern and the m/z ratios from the reaction products and the fragmentation processes. Based on these considerations, if we detect a signal at $m/z=53$, that is, the ion of the highest mass-to-charge ratio

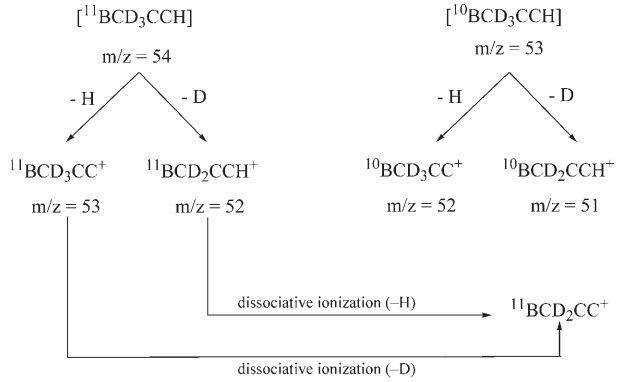

Figure 4. Schematic representation of the atomic hydrogen and deuterium loss pathways from two intermediates formed in the reactions of ^{11}B and ^{10}B with $CD_3CCH(X^1A_1)$. The corresponding *m/z* ratios are also indicated.

which can be formed in these experiments, we have an explicit verification of an atomic hydrogen loss pathway. This means the hydrogen atom is eliminated from the acetylenic group. A signal at $m/z=52$ could originate from $^{10}BC_3D_3^+$ and/or from $^{11}BC_3D_2H^+$.

As a matter of fact, reactive scattering signals were observed at $m/z=53$ and 52 (Figure 5-8). This demonstrates explicitly that at least the atomic hydrogen pathway is open and that

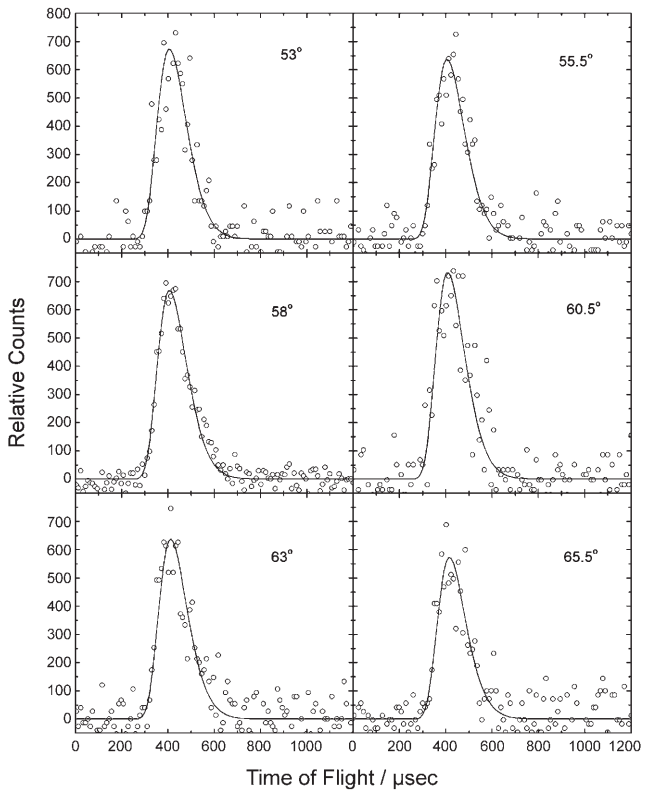

Figure 5. Time-of-flight data of the atomic hydrogen loss channel at $m/z=53$ recorded for the reaction $^{11}B(^2P_j)+CD_3CCH(X^1A_1)$ at various laboratory angles at a collision energy of 21.9 kJ mol^{-1}. The circles represent the experimental data, and the solid line the fits. Each TOF spectrum has been normalized to the relative intensity of each angle.

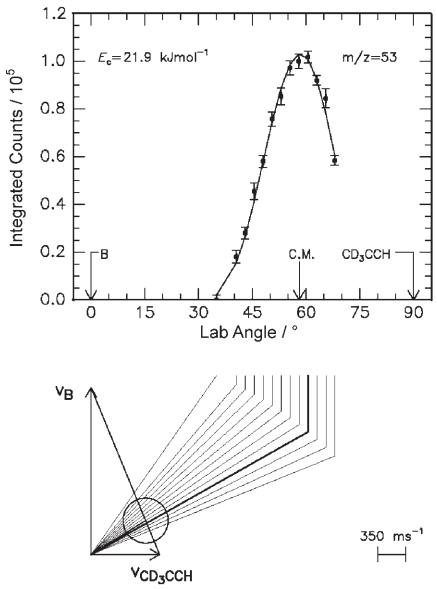

Figure 6. Lower panel: Newton diagram for the reaction $^{11}B(^2P_j)+CD_3CCH(X^1A_1)$ at a collision energy of 21.9 kJ mol^{-1}. Upper panel: Laboratory angular distribution of the $^{11}BC_3D_3$ product at $m/z=53$. Circles and 1σ error bars indicate experimental data, and the solid line indicates the calculated distribution. The center-of-mass angle is indicated by C.M. The solid lines originating in the Newton diagram point to distinct laboratory angles whose times of flight are shown in Figure 5.

the hydrogen atom is released from the acetylenic unit. In addition, the LAB distributions and TOF spectra of $m/z=53$ and 52 differ, suggesting that the atomic deuterium loss pathway is open.A fitting of the laboratory data substantiates this assumption. Data taken at $m/z=53$ could be assigned to a single reaction channel $^{11}BC_3D_3+H$ confirming that the atomic hydrogen channel is open (Figure 5 and Figure 6). However, TOFs and the LAB distributions at $m/z=52$ had to be fit with two components: a center-of-mass function of the atomic hydrogen loss channel of the ^{10}B reactant leading to $^{10}BC_3D_3^+$ and a second channel from the ^{11}B reactant leading via atomic deuterium emission from the [D3]methyl group to $^{11}BC_3D_2H$ (Figures 7 and 8). Figure 9 confirms that the atomic deuterium loss pathway is open. The center-of-mass functions of the atomic hydrogen and deuterium pathways, as discussed below, could also be utilized—after correcting for the reaction masses—to fit the data of the boron–methylacetylene system to a two-channel fit (Figure 2 and 3). Summarized, the data obtained from the reaction of ground-state boron atoms with [D3]methylacetylene verify the existence of two reaction pathways via hydrogen and deuterium atom loss from the acetylenic and methyl group, respectively, leading to molecules of the generic formulae $^{11}BC_3D_3$ and $^{11}BC_3D_2H$. It should be stressed that the use of (partially) deuterated reactants presents a valuable tool to investigate multiple channels arising from atomic hydrogen and/or deuterium elimination channels as demonstrated recently in our laboratory, for example, for the C/CD_3CCH,[36] C_2/CD_3CCH,[37] C_2D/CH_3CCH,[38] C_2D/CD_3CCH,[38] and C_3H_5/CD_3CCD,[39] C_3H_5/CD_3CCH,[39] and C_6H_5/CH_3CCD[40] systems.

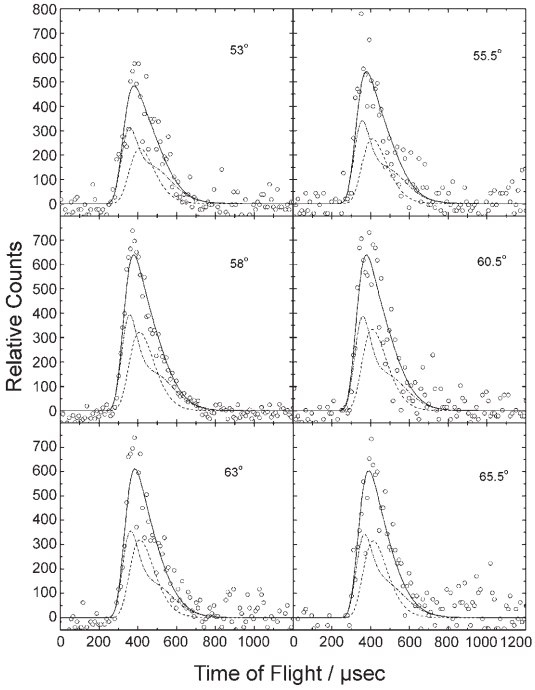

Figure 7. Time-of-flight data at $m/z = 52$ recorded for the reaction $^{11/10}B$-(^2P_j) + $CD_3CCH(X^1A_1)$ at various laboratory angles at a collision energy of 21.9 kJ mol^{-1}. The circles represent the experimental data, and the solid line the fit. The dashed lines represent two microchannels, the solid line the sum (dash: hydrogen loss; dash-dot: deuterium loss). Each TOF spectrum has been normalized to the relative intensity of each angle.

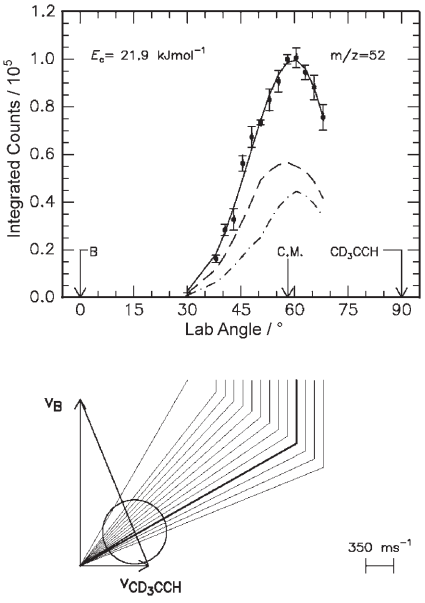

Figure 8. Lower panel: Newton diagram for the reaction $^{11/10}B(^2P_j) + CD_3CCH$-($X^1A_1$) at a collision energy of 21.9 kJ mol^{-1}. Upper panel: Laboratory angular distribution of the $^{11}BC_3D_2H$ (deuterium loss pathway) and $^{10}BC_3D_3$ products at $m/z = 52$ (fragmentation of the product formed via the hydrogen atom elimination pathway). Circles and 1σ error bars indicate experimental data, the solid line indicates the calculated distribution and the dashed lines represent two microchannels. The center-of-mass angle is indicated by C.M. The solid lines originating in the Newton diagram point to distinct laboratory angles whose times of flight are shown in Figure 7.

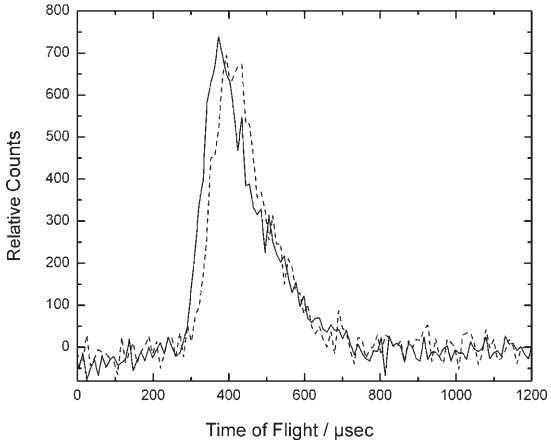

Figure 9. Overlaid TOF spectra at the center-of-mass angle as extracted from Figures 5 and 7 recorded at $m/z = 53$ (-----) and $m/z = 52$ (——). The different shapes of the TOF spectra are clearly visible.

2.2. Center-of-Mass Functions

Figures 10 and 11 display the center-of-mass translational energy distribution, $P(E_T)$, together with the center-of-mass angular distributions, $T(\theta)$s, for the atomic hydrogen and deuterium loss channels, respectively, to form the $^{11}BC_3D_3$ and $^{11}BC_3D_2H$ reaction products. The fits obtained accounted for the mass difference of the atomic boron reactant, that is, 11 vs. 10 amu. Best fits of the LAB distributions and the TOF data could be achieved with $P(E_T)$s extending to a maximum translational energy release (E_{max}) of 110–120 kJ mol^{-1} (H loss) and 94–108 kJ mol^{-1} (D loss). Due to the emission of a light deuterium and hydrogen atom, both high energy cutoffs are relatively insensitive; adding or subtracting up to 15 kJ mol^{-1} does not change the fit. Recall that E_{max} is the sum of the reaction exoergicity plus the collision energy. Therefore, by subtracting the

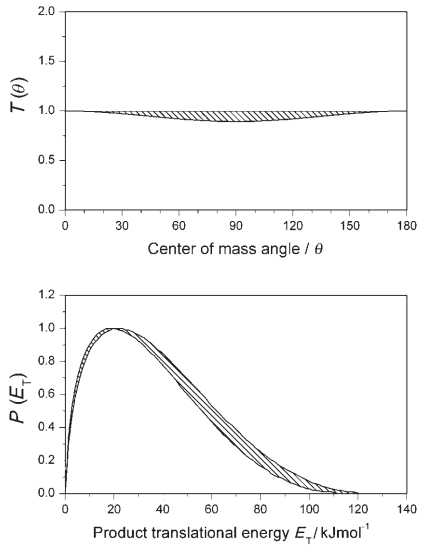

Figure 10. Center-of-mass translational energy flux (lower panel) and angular (upper panel) distributions for the reaction $^{11}B(^2P_j) + CD_3CCH(X^1A_1) \rightarrow$ $^{11}BC_3D_3 + H$ at a collision energy of 21.9 kJ mol^{-1}. The two lines limit the range of acceptable fits to within 1σ error bars.

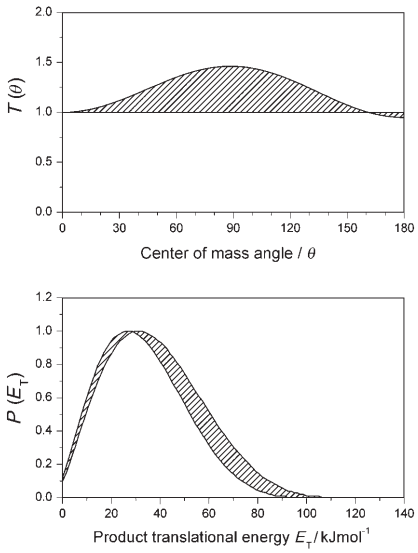

Figure 11. Center-of-mass translational energy flux (lower) and angular (upper) distributions for the reaction $^{11}B(^2P_j)+CD_3CCH(X^1A_1)\rightarrow{}^{11}BC_3D_2H+D$ at a collision energy of 21.9 kJ mol^{-1}. The two lines limit the range of acceptable fits to within 1σ error bars.

collision energy from the high energy cut-off, we are left with experimental exoergicities of 94 ± 15 kJ mol^{-1} and 80 ± 15 kJ mol^{-1}, respectively. These experimental data can be utilized later to be compared with ab initio calculations to identify the structural isomer(s) formed. Secondly, both $P(E_T)$s were found to peak away from zero translational energy at 15–25 kJ mol^{-1} and 20–30 kJ mol^{-1}. This pattern can account for two reaction scenarios. First—in the most ideal case—this peak indicates the existence of an exit transition state and hence a repulsive energy loss in the atomic hydrogen and deuterium pathways. Note that a barrier-less reaction is expected to result in a center-of-mass translational energy distribution peaking at or close to zero translational energy. Alternatively, even if a reaction has a loose exit transition state, the peaking away from zero translational energy could be the result of dynamical effects, for instance, a short lifetime of the decomposing reaction intermediates and possibly a more direct reaction mechanism.[41,42] This has been observed, for example, in the reaction of carbon atoms with phosphine (PH_3) studied recently in our laboratory.[43]

We would like to comment now on the center-of-mass angular distributions. Both distributions were found—within the error limits—to be symmetric around 90°. This finding implies that the lifetime(s) of the decomposing complex(es) is(are) longer than the rotational period. It should be stressed that within the uncertainties of the experiment, the H atom elimination pathway could be fit with either an isotropic or center-of-mass angular distribution holding a minimum at 90°. Likewise, the atomic deuterium loss pathway showed an isotropic fit; however, a distribution peaking at 90° could fit the data as well. Nevertheless, these findings indicate indirect scattering dynamics via the formation of $^{11}BC_3D3H$ reaction intermediates. In both cases, the relatively moderate polarization of the $T(\theta)$ can be understood in terms of total angular momentum conservation.[44] Here, most of the initial orbital angular momentum channels into the final rotational excitation of the reaction products, leading to a poor coupling between the initial and final orbital angular momentum. The branching ratio of the deuterium versus hydrogen loss channels was derived to be 2.2 ± 0.2. We would like to state explicitly that the natural $^{11}B/^{10}B$ abundance has been accounted for in the fits and in the derived branching ratio. It is important to note that we could also import the derived center-of-mass functions of the atomic hydrogen and deuterium loss pathways to fit the data of the $^{11}B(^2P_j)+CH_3CCH(X^1A_1)$ reaction with a two-channel fit (Figure 12). However, the branching ratios between two channels could be varied from 1.5:1 and 2.7:1 without having a significant effect on the fit as quantified by the χ^2 parameter of the fitting routing and a visual inspection of the TOFs and LAB distribution. It should be stressed that we were not able to fit the LAB distributions and TOF data with one channel without simultaneously decreasing the quality of the fit as based on the χ^2 parameter.

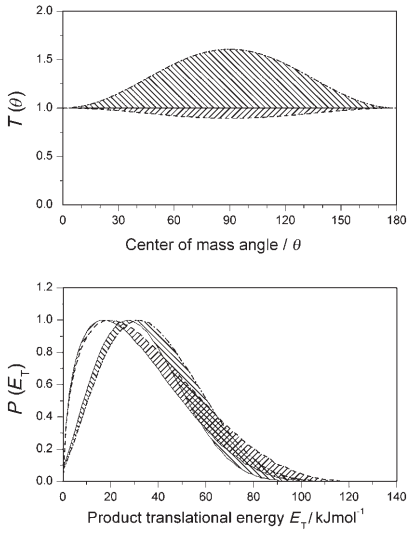

Figure 12. Center-of-mass translational energy flux (lower panel) and angular (upper panel) distributions for the reaction $^{11}B(^2P_j)+CH_3CCH(X^1A_1)\rightarrow{}^{11}BC_3H_3+H$ at a collision energy of 21.6 kJ mol^{-1}. The two lines limit the range of acceptable fits to within 1σ error bars.

It is interesting to address briefly the shape of the center-of-mass angular distribution together with angular momentum conservation of the title reactions. This system presents a traditional example where the initial orbital angular momentum is transformed mainly into the rotational excitation of the polyatomic reaction products. The total angular momentum J is given by Equation (2):

$$\mathbf{J}=\mathbf{L}+\mathbf{j}=\mathbf{L}'+\mathbf{j}' \qquad (2)$$

with the rotational angular momenta of the reactants and products **j** and **j**′ and the initial and final orbital angular momenta **L** and **L**′.[44] Since the reactant beams are prepared in a supersonic expansion, the rotational excitation of the reactant

molecules is expected to be small and Equation (2) can be simplified [Eq. (3)]:

$$\mathbf{J} \approx \mathbf{L} = \mathbf{L}' + \mathbf{j}' \quad (3)$$

Since kinetic experiments and our electronic structure calculations suggest that the reaction of atomic boron with methylacetylene has no entrance barrier and proceeds within orbiting limits, the maximum impact parameter b_{max} leading to a complex formation is approximated in terms of the classical capture theory to be between 3.0 and 3.4 Å.[45] The maximum orbital angular momentum $\mathbf{L}_{max}$ relates to b_{max} via Equation (4):

$$\mathbf{L}_{max} = \mu\, b_{max}\, v_r, \quad (4)$$

where μ is the reduced mass and v_r the relative velocity of the reactants. This would translate into $\mathbf{L}_{max}$ in the range of 110–130 $\hbar$. An upper limit of $\mathbf{L}'$ can also be estimated by assuming a relative velocity of the recoiling products corresponding to the average translational energy release $<E_T>$, and choosing an acetylenic C≡C-bond length of about 1.3 Å as the exit impact parameter. This calculates $\mathbf{L}'$ to be between 15–30 $\hbar$. Consequently, the initial orbital angular momentum is much larger than the final orbital angular momentum; most of the initial orbital angular momentum channels into rotational excitation of the polyatomic product, resulting in a relatively weakly polarized $T(\theta)s$. This weak **L**–**L**′ correlation is a direct result of large impact parameters contributing to the complex formation and the inability of the departing hydrogen/deuterium atoms to carry significant orbital angular momentum.

3. Discussion

3.1. Identification of Reaction Product(s)

To expose the actual reaction mechanism(s), we must first elucidate the reaction product(s). For this we compare the experimentally determined reaction energies with those of different isomers determined from ab inito calculations. The relative energies of the $^{11}BC_3H_3+H$ products together with the intermediates and transition states with respect to the atomic boron plus methylacetylene reactants, were obtained by coupled cluster CCSD(T)[46–49] calculations with cc-pVTZ basis functions at the B3LYP[50,51]/6-311(d,p) optimized geometries, including B3LYP/6-311G(d,p) zero point corrections. The Gaussian 98[52] program package was employed for the calculations. This computational approach is expected to provide accuracies of 5–10 kJ mol^{-1} for the relative energies (Figures 13 to 16). Figure 13 depicts the structures of the energetically accessible $^{11}BC_3H_3$ isomers. Recall that the translational energy distributions showed that the reaction channels are exoergic by 88 ± 15 kJ mol^{-1} and 78 ± 15 kJ mol^{-1}, respectively (Figure 12). We can now compare this data with the theoretical reaction energies. Here, four low lying $^{11}BC_3H_3$ isomers were located. The **p1** structure is the most stable isomer, and the reaction exoergicity to form **p1** + H is calculated to be 128 kJ mol^{-1}. The **p2** isomer is less stable by about 41 kJ mol^{-1} compared to **p1**. The

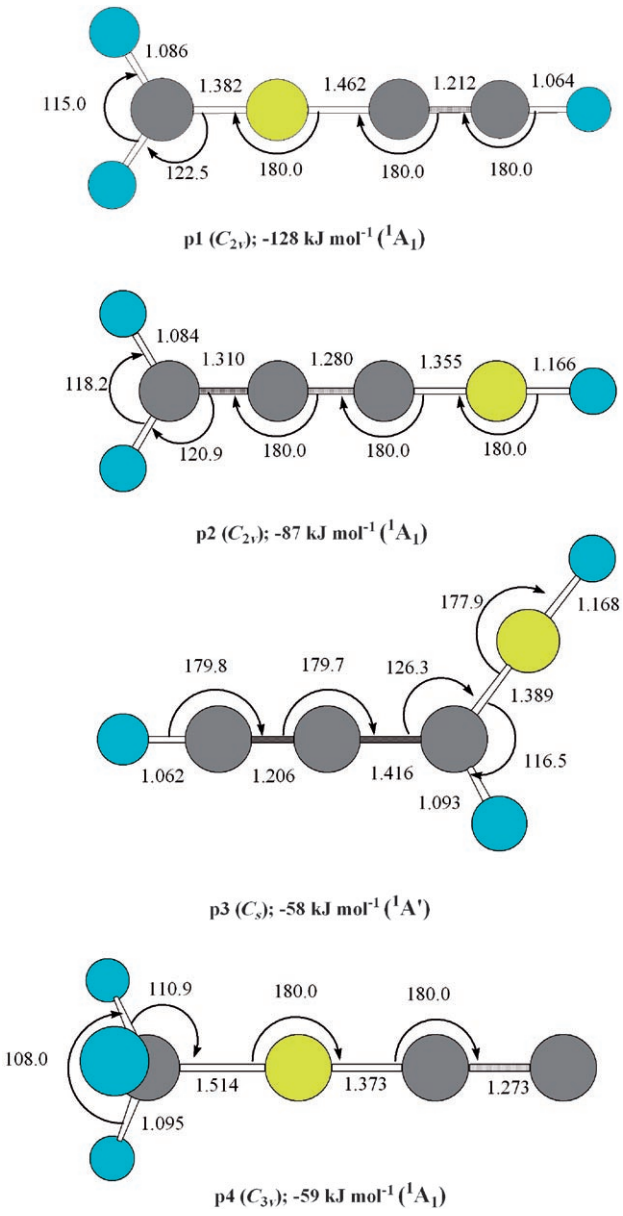

Figure 13. Structures of energetically accessible $^{11}BC_3H_3$ isomers; bond angles and lengths are given in degrees and Angstrom, respectively. Point groups are given in parenthesis. The energetics given present the exoergicities of the $^{11}BC_3H_3+H$ channel with respect to the separated atomic boron and methylacetylene reactants, respectively (yellow: boron; blue: hydrogen; black: carbon).

structures **p3** and **p4** are within the computational reliability and are isoenergetic and energetically less favorable by about 27 kJ mol^{-1} with respect to **p2**. By comparison of the experimental data with the ab initio values, **p2** is the most likely reaction product for the reaction; however, we cannot exclude additional contributions of **p3** and **p4** at the present stage. Based on this, we can compute the fraction of total energy channelled into the translational motion of the products to be 30–35 %. Also, we computed the reaction energies for the hydrogen atom and deuterium atom elimination pathways in the reaction of boron atoms with [D3]methylacetylene to form two isotopomers of **p2**, that is, the C_{2v} symmetric $D_2CCCBH(X^1A_1)$

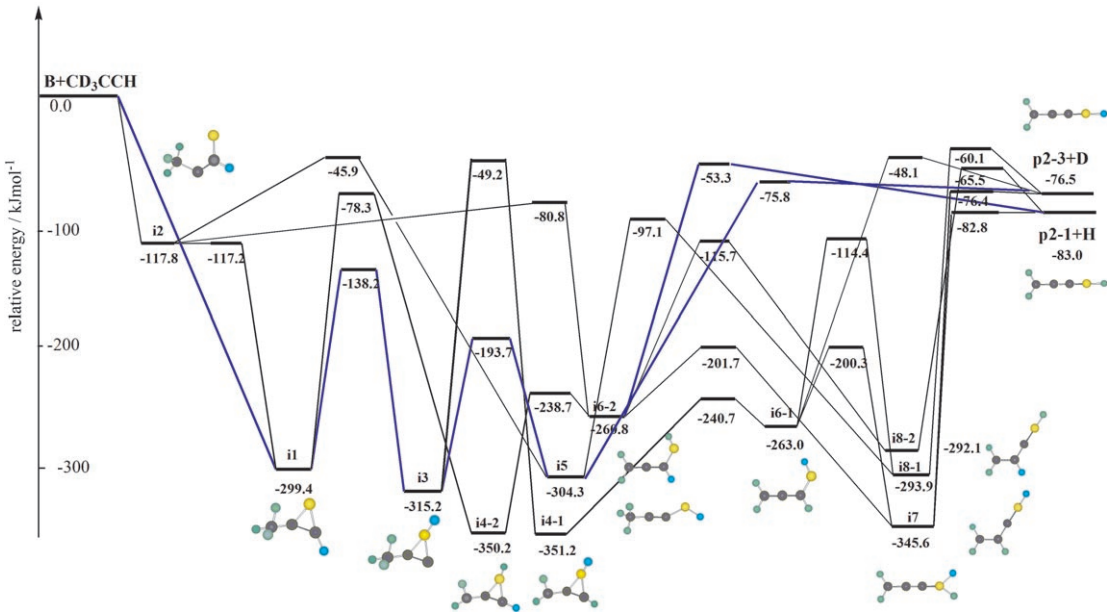

Figure 14. Computed potential energy surface of the reaction of ^{11}B with [D3]methylacetylene to form two isotopomers of the **p2** reaction product. The main reaction mechanisms are depicted in blue lines.

and $D_2CCCBD(X^1A_1)$ structures (Figure 14). The computed reaction energies of $-77\,kJ\,mol^{-1}$ and $-83\,kJ\,mol^{-1}$ correlate very nicely with the experimentally derived values of $-80\pm15\,kJ\,mol^{-1}$ and $-94\pm15\,kJ\,mol^{-1}$, respectively. Summarized, we can conclude that the reaction of atomic boron with [D3]methylacetylene leads to the formation of two **p2** isotopomers via atomic deuterium and hydrogen elimination channels: $D_2CCCBH(X^1A_1)$ (**p2-3**) and $D_2CCCBD(X^1A_1)$ (**p2-1**).

3.2. Mechanistic Information

We summarize now all the experimental information obtained and combine these with the results from the electronic structure calculations. This helps us derive the reaction mechanisms leading to the experimentally observed atomic hydrogen and deuterium loss pathways. Most importantly, the shapes of the $T(\theta)$s demonstrated indirect scattering dynamics for both microchannels and hence the existence of $^{11}BC_3D_3H$ intermediates; these structures are compiled in Figure 14; the corresponding $^{11}BC_3H_4$ intermediates are presented in Figures 15 and 16. The computations suggest that the boron atom can add to the carbon–carbon triple bond of the [D3]methylacetylene molecule forming two initial collision complexes. These are **i1,** via addition to both carbon atoms and **i2,** through an addition of the boron atom to the terminal carbon atom (α-carbon). The latter pathway is directed by the steric effect of the CD_3-group and the enhanced cone of acceptance of the α-carbon atom compared to the β-carbon atom (the carbon atom to which the D3-methyl group is connected). Recall that this scenario is similar to the initial addition of ground-state carbon atoms to the α-carbon atom of methylacetylene as found in the $C(^3P_j)+CH_3CCH$ and $C(^3P_j)+CD_3CCH$ systems.[36,53] The calculations predict that **i2** can isomerize easily to **i1**. Besides the initial collision complexes, the computations show that six additional intermediates (nine isotopomers in total) exist. In total, seven acyclic isotopomers can decompose via atomic hydrogen and deuterium elimination to form the experimentally observed **p2-1** and **p2-3** isotopomers, respectively. In detail, the intermediates **i5**, **i6-1**, **i7**, and **i8-1** can emit a deuterium atom via loose (**i5**, **i7**) or tight (**i6-1**, **i8-1**) exit transition states to yield **p2-3** + D. In this context, loose refers to exit barriers within the range of 0 up to a few $kJ\,mol^{-1}$, whereas tight exit transition state are those located at least $10\,kJ\,mol^{-1}$ (here: 18.4 and $17.5\,kJ\,mol^{-1}$) above the separated products. Also, three intermediates **i6-2**, **i7**, and **i8-2** can eject atomic hydrogen via loose (**i7**) and tight (**i6-2**, **i8-2**) exit transition states. Which of these reaction intermediates can be identified as the decomposing complex(es)? Considering the energy minimum path, boron can add to the terminal carbon atom to form **i2** which isomerizes to **i1**; alternatively, **i1** can be formed in a one-step addition process. This intermediate can isomerize via a hydrogen shift from the carbon to the boron atom forming **i3**; the latter can ring open to **i5**. This structure can loose a deuterium atom via a loose exit transition state or isomerizes to **i8-1** which in turn can emit a deuterium atom through a tight exit transition state. Based on the transition states involved, the deuterium emission from **i5** should be the preferential pathway. How about the structures **i6-1** and **i7**? The intermediate **i7** can be formed from **i6-2** and **i6-1**. However, based on the calculations, **i6-1** undergoes preferentially a deuterium atom elimination and **i6-2** emits a hydrogen atom. Therefore, **i7** is expected to play only a minor role in the scattering dynamics since its potential precursor complexes favor atomic hydrogen/deuterium emission pathways. Considering **i6-1**, this intermediate can only be formed from **i4-1**. The latter, however, is difficult to access. Its precursor—intermedi-

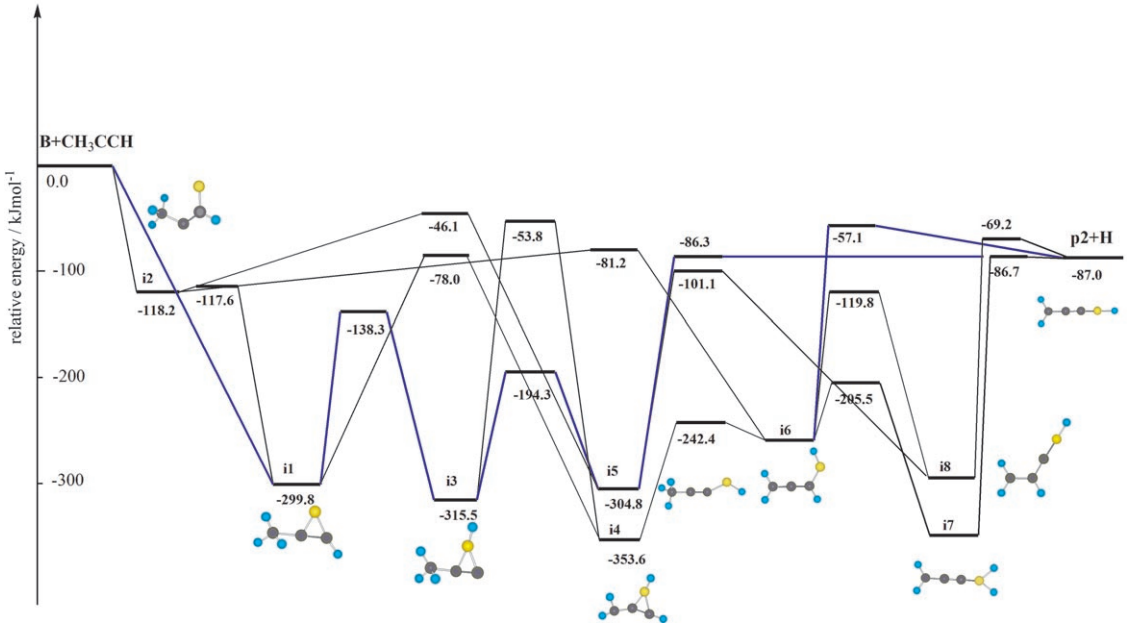

Figure 15. Computed potential energy surface of the reaction of ^{11}B with methylacetylene to form the **p2** reaction product. The main reaction mechanisms are depicted in blue lines.

ate **i1**—rather isomerizes to **i3** which in turn goes to **i5**. Therefore, if the reaction follows the lowest energy pathways, we would expect that **i1**→**i3**→**i5**→**p2-3** + D presents the dominating contribution to the D atom loss pathway followed by **i1**→**i3**→**i5**→**i8-1**→**p2-3** + D. We also conducted a brief Rice–Ramsperger–Kassel–Marcus (RRKM) study of this system.[54,55] This approach computes individual rate constants and product branching ratios within the limit that the energy of the decomposing intermediate is completely randomized. The RRKM calculations predict that the reaction sequence **i1**→**i3**→**i5**→**p2-3** + D presents the dominating reaction pathway. In the limit of complete energy randomization, branching ratios of the D versus the H loss were computed to be about 2000:1. Clearly, this contradicts the experimental findings of a branching ratio of 2.2 ± 0.2:1; recall that we observed the D loss pathway (via the reaction sequence **i1**→**i3**→**i5**→**p2-3** + D) and also the H atom loss channel. Consequently, the hydrogen loss pathway is likely the result of the reaction channel following a non-RRKM behavior. This pattern is also followed on the related $^{11}B/CH_3CCH$ surface. Here, RRKM calculations suggest that the reaction proceeds via the reaction sequence **i1**→**i3**→**i5**→**p2** + H.

We would like to investigate now the possible contributors to the atomic hydrogen loss channel which can account for the non-RRKM behavior of this reaction. Recall that three intermediates are feasible candidates (**i6-2**, **i7**, and **i8-2**). Both latter structures can only be formed via isomerization of **i6-2**. Considering the energetics, **i6-2** is therefore expected to fragment via atomic hydrogen loss to **p2-1** rather then undergoing rearrangements to **i7** and **i8-2**. However, the formation of the intermediate **i6-2** itself presents an interesting issue. A closer look at the potential energy surface (Figure 14) suggests two feasible reaction pathways, that is, **i2**→**i6-2** and **i2**→**i1**→**i4-2**→**i6-2**. Considering the initial addition of the boron atom to the terminal carbon atom to form **i2**, a statistical reaction would proceed through the lowest energy pathway via ring closure to **i1**. However, the competing pathway **i2**→**i6-2**, which is not favorable under RRKM conditions, requires a non-statistical nature of this microchannel. The latter could decompose then via a hydrogen atom ejection to form **p2-1**. Summarized, the experimental data combined with electronic structure and statistical calculations suggests that the reaction involves at least two reaction pathways; the atomic deuterium emission channel follows a statistical pattern and the reaction sequence **i1**→**i3**→**i5**→**p2-3** + D. On the other hand, the experimental observation of the atomic hydrogen loss can only be accounted for by a non-statistical channel via the intermediate **i6-2**.

3.3. Formation of Alternative $^{11}BC_3H_3$ Isomers

We attempt now to investigate why isomers **p1**, **p3** and **p4**, are—only minor reaction products—if at all present. In order for **p1** to be formed, it is crucial that the methyl group migrates in intermediate **i1** from the carbon atom to the boron atom. This process can be followed by a ring opening and emission of a hydrogen atom from the [D3]methyl group to form **p1** or an elimination of atomic hydrogen to form **p4**. However, the rate-limiting step in this reaction sequence is likely the migration of the heavy [D3]methyl group; the competing hydrogen and deuterium migrations are expected—due to the lower mass of the migrating species—to be faster (Figures 14 and 15). Summarized, the facile atomic migration is expected to effectively eliminate the synthesis of **p1** and **p4**. Note that the hindered migration of the [D3]methyl group was

also found to dictate the formation of the final reaction products in the reaction of atomic boron with dimethylacetylene.[28] Finally, the formation of **p3** requires an initial insertion of atomic boron into a carbon–hydrogen bond of the [D3]methyl group followed by a deuterium atom emission. As shown previously in the crossed beam reactions of boron atoms with benzene,[25–27] dimethylacetylene,[28] ethylene,[22] and acetylene,[23,24] insertion reactions do not take place. Likewise, we conducted experiments of atomic boron with methane at a collision energy of about 25 kJ mol^{-1}, with no reactive scattering signal observed.[56] This suggests that an insertion of atomic boron into carbon–hydrogen bonds is an unlikely reaction mechanism.

Table 2. Alternative reaction channels and their energetics in the reaction of boron atoms with methylacetylene.

Channel	Reaction products	Reaction energy [kJ mol^{-1}]
1	$C(^3P_j) + BC_2H_4(X^2B_2)$	367
2	$CH(X^2\Pi) + BC_2H_3(X^1A_1)$	104
3	$CH_2(a^1A_1) + BC_2H_2(X^2B_2)$	131
4	$CH_3(X^2A_2'') + BC_2H(X^3\Sigma^-)$	−37
5	$CH_4(X^1A_1) + BC_2(X^4\Sigma^-)$	−109
6	$C_2(X^1\Sigma_g^+) + BCH_4(X^2A')$	358
7	$C_2H(X^2\Sigma^+) + BCH_3(X^1A_1)$	175
8	$C_2H_2(X^1A_1) + BCH_2(X^2A_1)$	102
9	$C_2H_3(X^2A') + BCH(X^3\Sigma^-)$	229
10	$C_2H_4(X^1A_1) + BC(X^4\Sigma^-)$	123
11	$C_3H(X^2A') + BH_3(X^1A_1)$	−204
12	$C_3H_2(X^1A_1) + BH_2(X^2A_1)$	−50
13	$C_3H_3(X^2B_1) + BH(X^1\Sigma^+)$	9

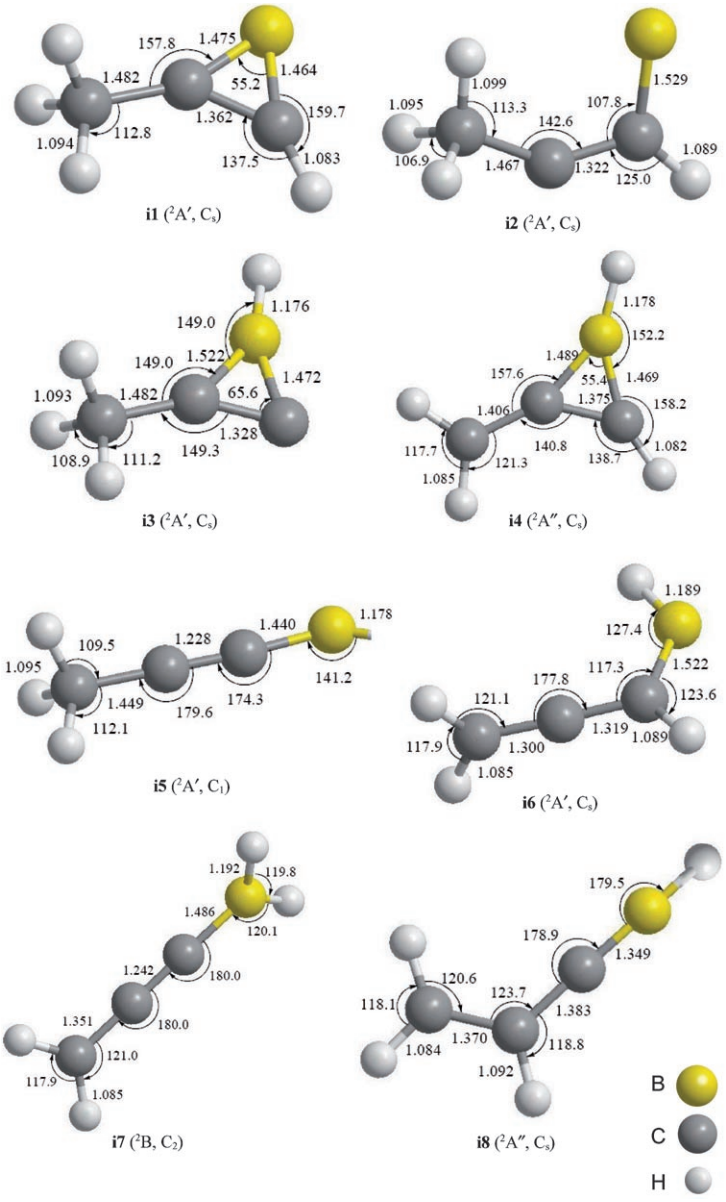

Figure 16. Structures of energetically accessible $^{11}BC_3H_4$ intermediates; bond angles and lengths are given in degrees and Angstrom, respectively. Point groups are given in parenthesis (yellow: boron; gray: hydrogen; black: carbon).

3.4. Alternative Exit Channels

We also investigated the existence of alternative exit channels as summarized in Table 2. Among these pathways, only channels 4, 5, and 11–13 are energetically accessible under our experimental conditions. The existence of channels 4 and 5 should be reflected in a reactive scattering signal at $m/z = 35$ and 34, that is, $^{10}BC_2H^+$ ($m/z = 35$), $^{11}BC_2^+$ ($m/z = 35$), and $^{10}BC_2^+$ ($m/z = 34$). These mass-to-charge ratios are essentially background-free. However, no reactive scattering signal was observed at $m/z = 35$ and 34. The involvement of channels 11–13 is a tricky problem. We investigated the existence of $m/z = 11$, that is, $^{10}BH^+$. Only the signal from elastically/inelastically scattered boron atoms $m/z = 11$ could be monitored. Considering the structures of the intermediates involved, we would expect only channel 13 to be open. However, considering the strongly exoergic competing reaction to form the **p2** isomer of $^{11}BC_3H_3$, channel 13 is expected to be only of minor importance at the most. Considering the strongly exoergic channels 5 and 11, we would like to stress that no reaction intermediate can connect to the borane and tricarbon hydride radical. Also, the formation of methane and dicarbon boride (channel 5) can only occur from intermediate **i5** via a highly strained, tight five-membered transition state; this pathway would be therefore less favorable compared to the atomic hydrogen emission.

4. Conclusions

The reactions of ground-state boron atoms, $B(^2P_j)$, with methylacetylene, $CH_3CCH(X^1A_1)$, and its [D3]-substituted isotopomer were studied under single collision conditions using the crossed molecular beam technique. Utilizing the CD_3CCH reactant, we could extract important information on the reaction dynamics involved. The reaction follows indirect scattering dynamics and proceeds at least through two

reaction channels via atomic deuterium and hydrogen atom elimination pathways. They lead ultimately to the formation of two isotopomers, that is, the C_{2v} symmetric D_2CCCBH and D_2CCCBD structures. The atomic deuterium replacement channel could be explained in terms of the statistical, unimolecular decomposition of a reaction intermediate **i5** and the involvement of the reaction sequence **i1**→**i3**→**i5**→**p2-3** + D, whereas the atomic hydrogen loss pathway can only be accounted for with a non-RRKM behavior of the system through intermediate **i6-2**.

Acknowledgements

This work was supported by the Air Force Office of Scientific Research (AFOSR; W911NF-05-1-0448). The authors would like to thank Ed Kawamura (University of Hawaii, Department of Chemistry) for his electrical work. CHK and AHHC want to thank the National Center for High Performance Computer in Taiwan for the support of computer resources.

Keywords: boron · gas-phase reactions · laser spectroscopy · molecular dynamics · reaction mechanisms

[1] J. M. Mota, J. Abenojar, M. A. Martinez, F. Velasco, A. J. Criado, *J. Solid State Chem.* **2004**, *177*, 619–627.
[2] P. Politzer, P. Lane, M. C. Concha, *J. Phys. Chem. A* **1999**, *103*, 1419–1425.
[3] A. Ulas, K. K. Kuo, C. Gotzmer, *Combust. Flame* **2001**, *127*, 1935–1957.
[4] E. L. Dreizin, D. G. Keil, W. Felder, E. P. Vicenzi, *Combust. Flame* **1999**, *119*, 272–290.
[5] N. Metzler, H. Noeth, *Chem. Ber.* **1995**, 128, 711–717.
[6] K. C. Schadow, K. J. Wilson, E. Gutmark, R. A. Smith, *Combust. Boron-based Solid Propellants, Solid Fuel* **1993**, *7*, 402–411.
[7] I. M. E. Volpin, Y. D. Koreshkov, V. G. Dulova, D. N. Kursanov, *Tetrahedron* **1962**, *18*, 107–122.
[8] K. Krogh-Jespersen, D. Cremer, J. D. Dill, J. A. Pople, P. v. R. Schleyer, *J. Am. Chem. Soc.* **1981**, *103*, 2589–2594.
[9] O. Halova, *Sbornik Vysoke Skoly Chemicko-Technologicke v Praze, P: Fyzika Materialu a Merici Technika*, **1991**, P12, 5–14.
[10] Y. G. Byun, S. Saebo, C. U. Pittman, Jr., *J. Am. Chem. Soc.* **1991**, *113*, 3689–3696.
[11] P. H. M. Budzelaar, A. J. Kos, T. Clark, P. v. R. Schleyer, *Organometallics* **1985**, *4*, 429–437.
[12] J. R. Flores, A. Largo, *J. Phys. Chem.* **1992**, *96*, 3015–3021.
[13] T. Shirasaki, A. Derre, M. Menetrier, A. Tressaud, S. Flandrois, *Carbon* **2000**, *38*, 1461–1467.
[14] C. Poon, P. M. Mayer, *Can. J. Chem.* **2002**, *80*, 25–30.
[15] W.-H. Fang, S. D. Peyerimhoff, *Mol. Phys.* **1998**, *93*, 329–339.
[16] L. Andrews, P. Hassanzadeh, J. M. L. Martin, P. R. Taylor, *AIP Conf. Proc.* **1993**, *288*, 137 – 140.
[17] L. Andrews, P. Hassanzadeh, J. M. L. Martin, P. R. Taylor *J. Phys. Chem.* **1993**, 97, 5839–5847.
[18] J. M. L. Martin, P. R. Taylor, P. Hassanzadeh, L. Andrews, *J. Am. Chem. Soc.* **1993**, *115*, 2510–2511.
[19] D. V. Lanzisera, P. Hassanzadeh, Y. Hannachi, L. Andrews, *J. Am. Chem. Soc.* **1997**, *119*, 12402–12403.
[20] L. Andrews, D. V. Lanzisera, P. Hassanzadeh, Y. Hannachi, *J. Phys. Chem. A* **1998**, *102*, 3259–3267.
[21] N. Galland, Y. Hannachi, D. V. Lanzisera, L. Andrews, *Chem. Phys.* **1998**, *230*, 143–151.
[22] N. Balucani, O. Asvany, Y. T. Lee, R. I. Kaiser, N. Galland, Y. Hannachi, *J. Am. Chem. Soc.* **2000**, *122*, 11234–11235.
[23] N. Balucani, O. Asvany, Y. T. Lee, R. I. Kaiser, N. Galland, M. T. Rayez, Y. Hannachi, *J. Comput. Chem.* **2001**, *22*, 1359–1365.
[24] R. I. Kaiser, N. Balucani, N. Galland, F. Caralp, M. T. Rayez, Y. Hannachi, *Phys. Chem. Chem. Phys.* **2004**, *6*, 2205–2210.
[25] H. F. Bettinger, R. I. Kaiser, *J. Phys. Chem. A* **2004**, *108*, 4576–4586.
[26] R. I. Kaiser, H. F. Bettinger, *Angew. Chem.* **2002**, *114*, 2456–2458; *Angew. Chem. Int. Ed.* **2002**, *41*, 2350–2352.
[27] F. Zhang, Y. Guo, X. Gu, R. I. Kaiser, *Chem. Phys. Lett.* **2007**, *440*, 56–63.
[28] D. Sillars, R. I. Kaiser, N. Galland, Y. Hannachi, *J. Phys. Chem. A* **2003**, *107*, 5149–5156
[29] D. J. Pasto, *J. Am. Chem. Soc.* **1988**, *110*, 8164–8175.
[30] X. Gu, Y. Guo, R. I. Kaiser, *Int. J. Mass Spec.* **2005**, *246*, 29–34.
[31] X. B. Gu, Y. Guo, H. Chan, E. Kawamura, R. I. Kaiser, *Rev. Sci. Instrum.* **2005**, *76*, 116 103/116 101–116 103/116 103.
[32] X. B. Gu, Y. Guo, E. Kawamura, R. I. Kaiser, *Rev. Sci. Instrum.* **2005**, *76*, 083 115/083 111–083 115/083 116.
[33] X. Gu, Y. Guo, E. Kawamura, R. I. Kaiser, *J. Vac. Sci. Technol. A* **2006**, *24*, 505–511.
[34] M. Vernon, Ph.D., University of California, Berkley, **1981**.
[35] M. S. Weiss, Ph.D., University of California, Berkley, **1986**.
[36] R. I. Kaiser, A. M. Mebel, Y. T. Lee, A. H. H. Chang, *J. Chem. Phys.* **2001**, *115*, 5117–5125.
[37] X. Gu, Y. Guo, F. Zhang, A. M. Mebel, R. I. Kaiser, *Faraday Discuss.* **2006**, *133*, 245–275.
[38] R. I. Kaiser, C. C. Chiong, O. Asvany, Y. T. Lee, F. Stahl, P. v. R. Schleyer, H. F. Schaefer, III, *J. Chem. Phys.* **2001**, *114*, 3488–3496.
[39] Y. Guo, A. M. Mebel, F. Zhang, X. Gu, R. I. Kaiser, *J. Phys. Chem. A* **2007**, *111*, 4914–4921.
[40] R. I. Kaiser, O. Asvany, Y. T. Lee, H. F. Bettinger, P. v. R. Schleyer, H. F. Schaefer, III, *J. Chem. Phys.* **2000**, *112*, 4994–5001.
[41] R. I. Kaiser, *Chem. Rev.* **2002**, *102*, 1309–1358.
[42] R. I. Kaiser, A. M. Mebel, *Int. Rev. Phys. Chem.* **2002**, *21*, 307–356.
[43] Y. Guo, X. Gu, F. Zhang, B. J. Sun, M. F. Tsai, A. H. H. Chang, R. I. Kaiser, *J. Phys. Chem. A* **2007**, *111*, 3241–3247.
[44] W. B. Miller, S. A. Safron, D. R. Herschbach, *Discuss. Faraday Soc.* **1967**, *44*, 108–122.
[45] R. D. Levine, *Molecular Reaction Dynamics*, Cambridge University Press, Cambridge, **2005**.
[46] J. A. Pople, M. Head-Gordon, K. Raghavachari, *J. Chem. Phys.* **1987**, *87*, 5968–5975.
[47] G. D. Purvis, III, R. J. Bartlett, *J. Chem. Phys.* **1982**, *76*, 1910–1918.
[48] G. E. Scuseria, C. L. Janssen, H. F. Schaefer, III, *J. Chem. Phys.* **1988**, *89*, 7382–7387.
[49] G. E. Scuseria, H. F. Schaefer, III, *J. Chem. Phys.* **1989**, *90*, 3700–3703.
[50] A. D. Becke, *J. Chem. Phys.* **1993**, *98*, 5648–5652.
[51] C. Lee, W. Yang, R. G. Parr, *Phys. Rev. B* **1988**, *37*, 785–789.
[52] Gaussian 98 (Revision A5), M. J. Frisch, G. W. Trucks, H. B. Schlegel, G. E. Scuseria, M. A. Robb, J. R. Cheeseman, V. G. Zakrzewski, J. J. A. Montgomery, R. E. Stratmann, J. C. Burant, S. Dapprich, J. M. Millam, A. D. Daniels, K. N. Kudin, M. C. Strain, O. Farkas, J. Tomasi, V. Barone, M. Cossi, R. Cammi, B. Mennucci, C. Pomelli, C. Adamo, S. Clifford, J. Ochterski, G. A. Petersson, P. Y. Ayala, Q. Cui, K. Morokuma, D. K. Malick, A. D. Rabuck, K. Raghavachari, J. B. Foresman, J. Cioslowski, J. V. Ortiz, A. G. Baboul, B. B. Stefanov, A. L. G. Liu, P. Piskorz, I. Komaromi, R. Gomperts, R. L. Martin, D. J. Fox, T. Keith, M. A. Al-Laham, C. Y. Peng, A. Nanayakkara, C. Gonzalez, M. Challacombe, P. M. W. Gill, B. G. Johnson, W. Chen, M. W. Wong, J. L. Andres, M. Head-Gordon, E. S. Replogle, J. A. Pople; Gaussian, Inc., Pittsburgh PA, **1998**.
[53] R. I. Kaiser, D. Stranges, Y. T. Lee, A. G. Suits, *J. Chem. Phys.* **1996**, *105*, 8721–8733.
[54] H. Eyring, S. H. Lin, S. M. Lin, *Basis Chemical Kinetics*, Wiley, New York, **1980**.
[55] K. S. Noll, H. A. Weaver, P. D. Feldman, *Molecular Reaction Dynamics*, Cambridge University Press, New York, **1996**.
[56] R. I. Kaiser, unpublished results.

Received: July 24, 2007
Revised: October 5, 2007
Published online on December 20, 2007

